

# Crystal Growth and Seebeck Coefficient Measurement of $\text{HgBa}_2\text{CuO}_{4+\delta}$

Jingnan Cai

University of Minnesota, Twin Cities

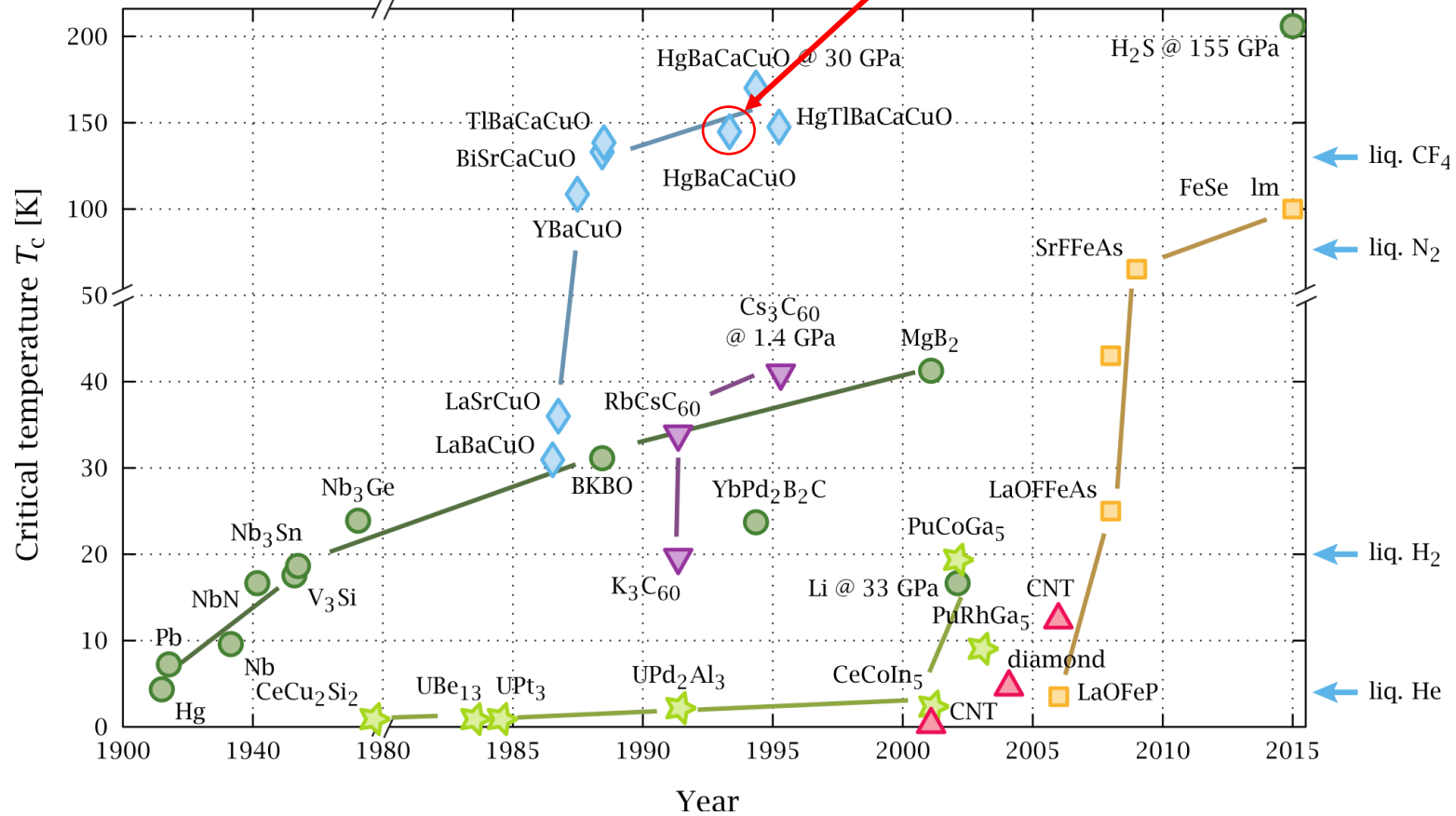
School of Physics and Astronomy

Thesis Advisor: Martin Greven

# Outline

- Introduction to Superconductivity
- $\text{HgBa}_2\text{CuO}_{4+\delta}$  (Hg1201)
- Crystal Growth and Characterization
- Seebeck Effect
- Seebeck Coefficient Measurement
- Conclusion

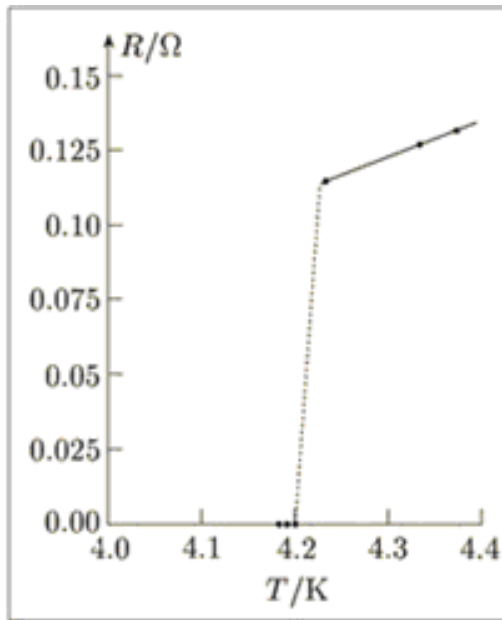
# History of Superconductivity



Timeline of superconductors. Copied from [1]

# History of Superconductivity

- First observed by H. K. Onnes in Hg while cooled down to 4.2K in the year of 1911.
- Zero Resistance



Data adopted from Onnes original paper [2].

- Meissner Effect
  - Type-I versus type-II

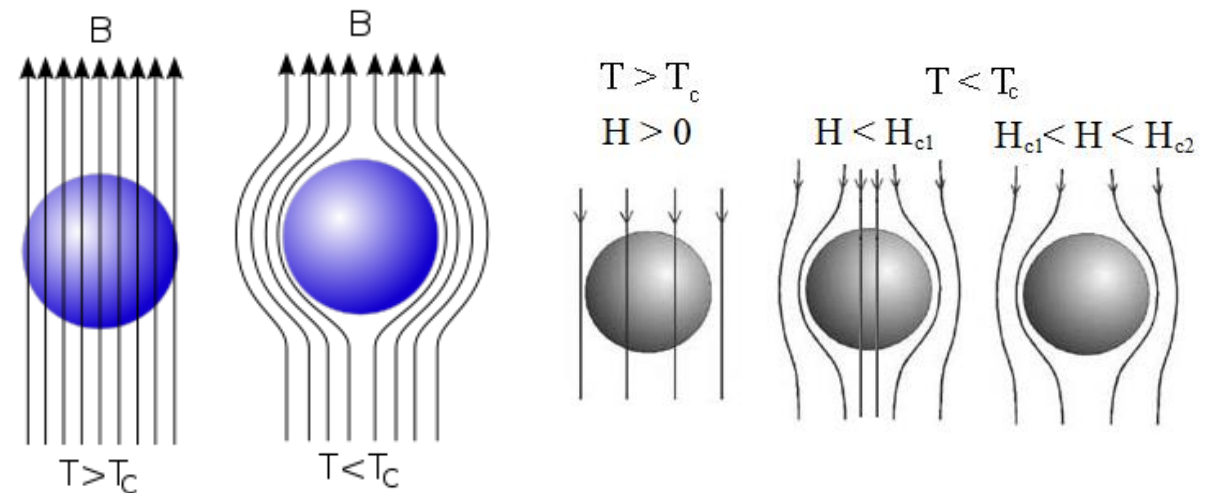


Diagram of Meissner effect in Type-I superconductor.  
<https://commons.wikimedia.org/wiki/File:EfektMeisnera.svg>

Diagram of Meissner effect in Type-II superconductor.  
<http://jeppejuul.com/research/projects/estimation-and-measurement-of-ac-losses-in-bi2sr2ca2cu3o10x-multifilament-tapes-and-one-layer-single-phase-cables/>

# Theory of Superconductivity

- Conventional Superconductors (Type-I)
  - Bardeen-Cooper-Schrieffer (BCS) Theory in 1957
    - Superconductivity caused by the Bose-Einstein condensation of Cooper pairs
    - Some types of attractive interactions between electrons
    - One example: phonon-mediated Cooper pairs

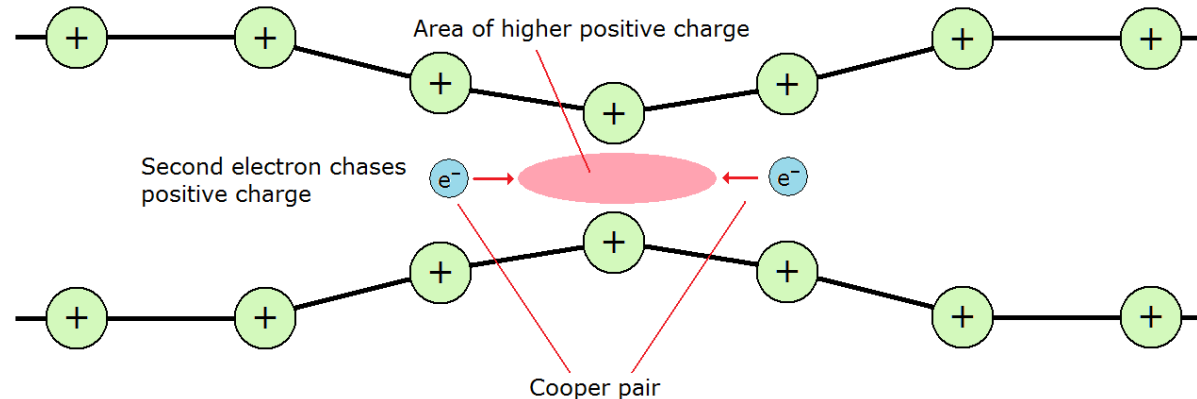
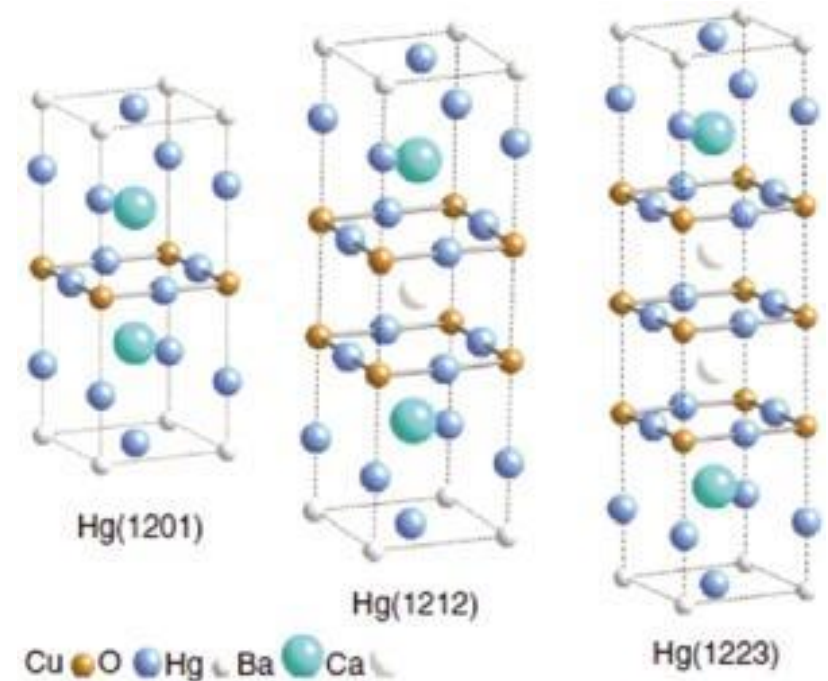


Diagram of Cooper pairs formed by the attraction between two electrons through positive ion lattice. Copied from [3]

# Superconducting Cuprates

- Superconductivity in cuprates is first discovered by J.G. Bednorz and K. A. Müller in Ba-La-Cu-O system in the Year of 1986 [4].
- Key feature:  $\text{CuO}_2$  plane
- Model compound:  $\text{HgBa}_2\text{CuO}_{4+\delta}$  (Hg1201)
  - Simple Tetragonal Structure
  - High  $T_c \approx 97\text{K}$



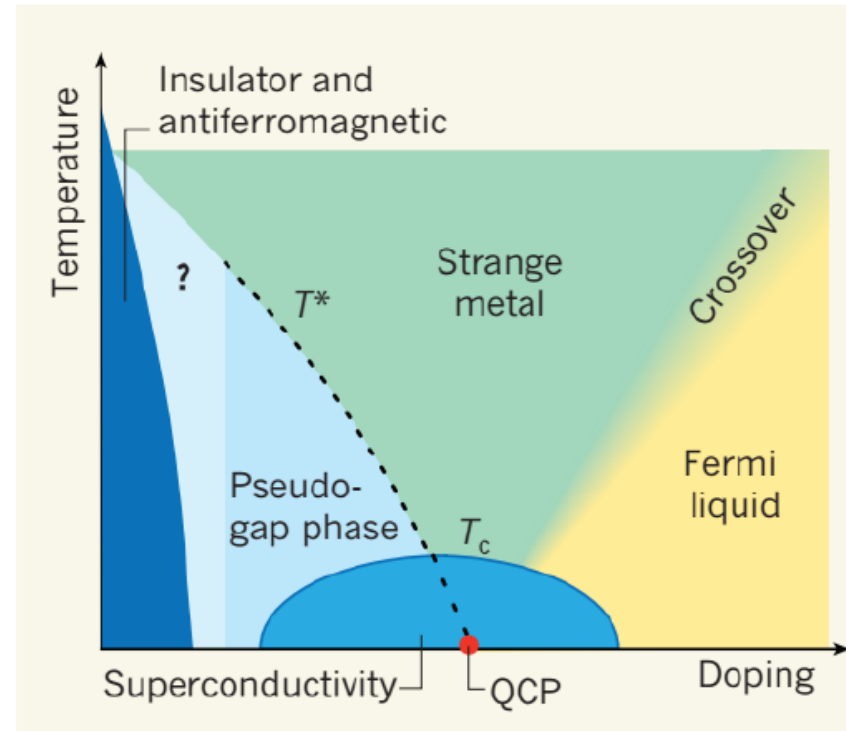
Crystal structures of three Hg-based cuprates. Copied from [5]

# Theory of Superconductivity

- Beyond BCS model: Unconventional Superconductivity
  - Loop Current Order
  - Quantum Criticality
  - Resonating Valence Band

# Theory of Superconductivity

- Phase Diagram

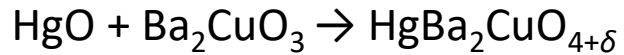
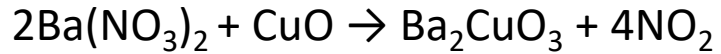


Phase diagram of Hole-doped cuprates.  
Copied from [6]



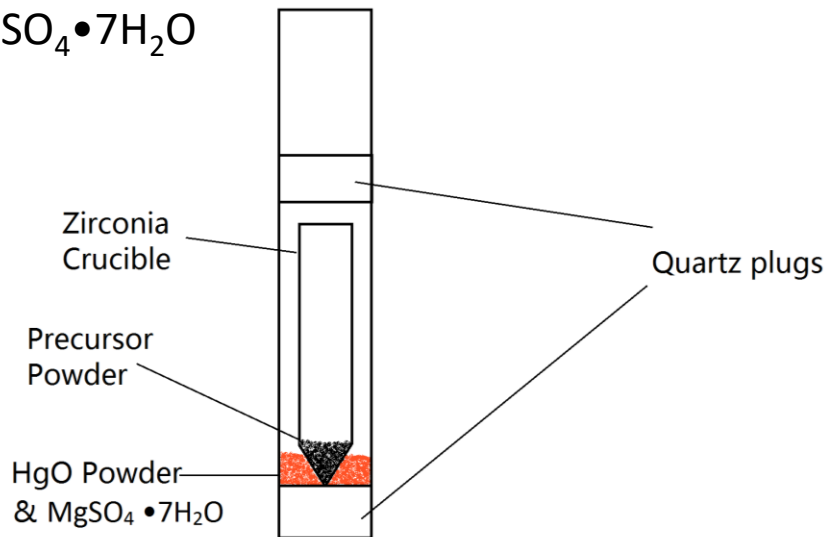
# Crystal Growth

Main Reactions:

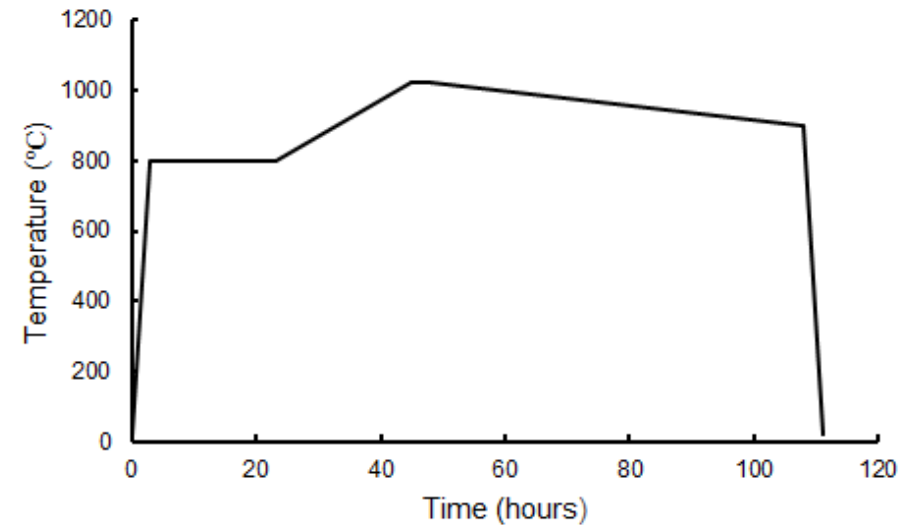


Optimized Growth Condition:

- 20h reaction time
- 30mg  $\text{MgSO}_4 \cdot 7\text{H}_2\text{O}$



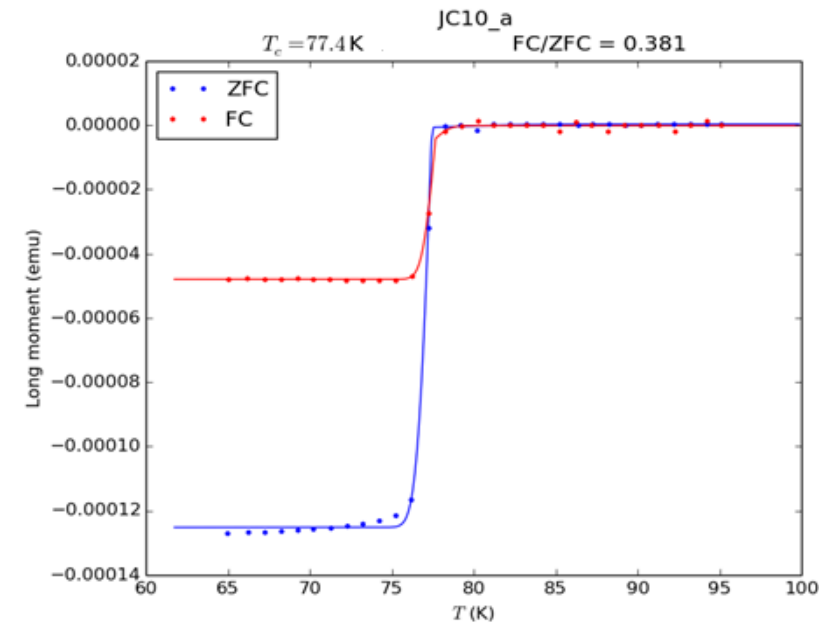
Schematic diagram for growth setup. The quartz plugs on both sides were welded to provide the vacuum sealing.



Temperature profile of the furnace. The reaction occurs at 800°C. The products are then molten at 1020 °C. The mixture is then cooled down at the rate of 2 °C/h for the crystallization of Hg1201.

# Magnetization Characterization

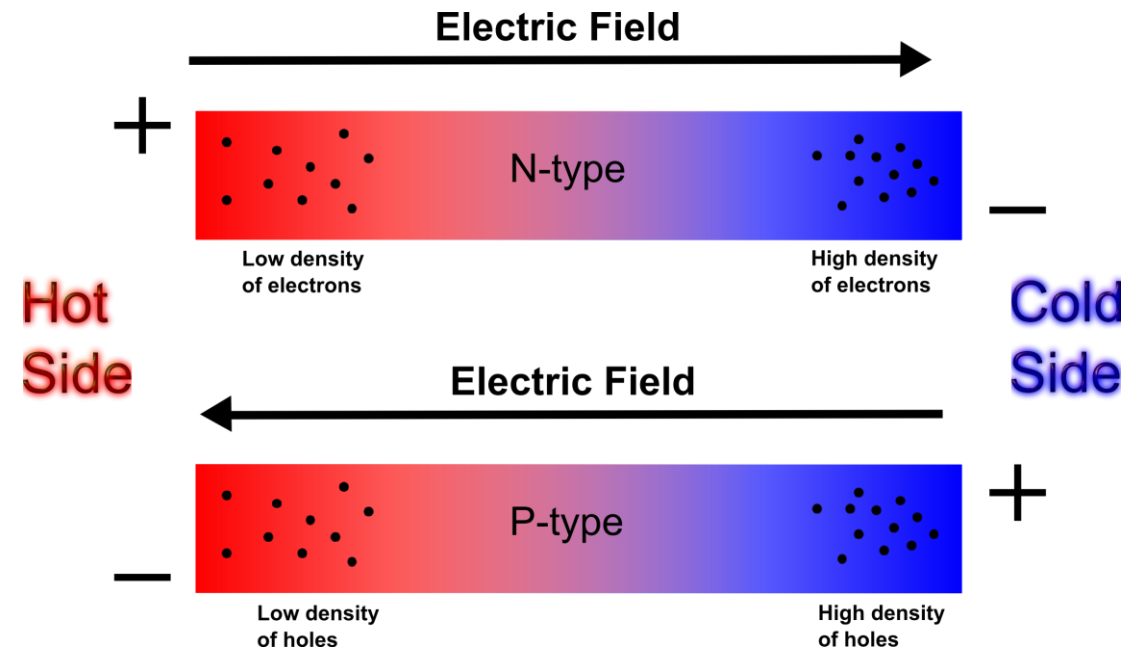
- Characterization done in MPMS (Magnetic Property Measurement System) from Quantum Design, Inc.
- Steps for characterization:
  - Cooling below  $T_c$  in zero field (ZFC)
  - Applying external field of 5 gauss
  - Measuring the magnetization while increasing the temperature over  $T_c$
  - Cooling down with magnetic field (FC)
  - Repeating the measurement in ZFC



The magnetization curve for an as-grown sample in ZFC-FC measurement. The sharp transition and high FC-ZFC ratio is the indication of high sample quality.

# Seebeck Effect

- Voltage induced by a temperature gradient
- $S = -\frac{\Delta V}{\Delta T}$  at equilibrium
- Seebeck Coefficient (Thermoelectric Power) has implications on density of states, the diffusion rate and the sign of the charge carrier.



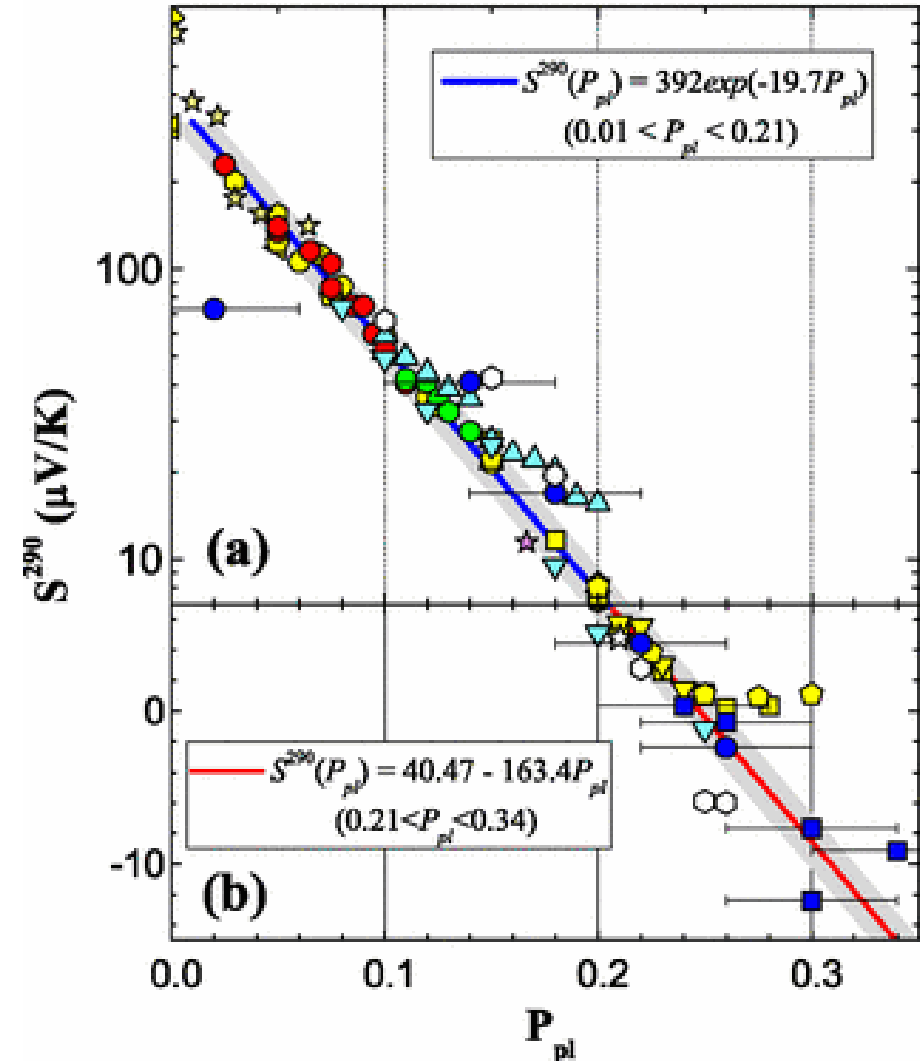
Pictorial depiction of Seebeck Effect.  
<http://www.mn.uio.no/fysikk/english/research/projects/bate/thermoelectricity/>

# Seebeck Effect

- Two principle mechanisms:
  - Thermal Diffusion of charge carriers
    - Microscopic picture:  
hot end has larger spread of energy levels  
→ higher concentration of high energy carriers and lower concentration of low energy carriers  
→ two competing diffusive current: high energy carriers from hot to cold end and the low energy carriers from cold to hot end  
→ a net current is induced when the two drifts rate are unequal
  - Phonon Drag
    - Phonon-electron interaction, prominent at  $T \approx \frac{\theta_D}{5}$ , since phonon-phonon scattering is more prominent at higher temperature, and phonon density is small on low temperature
    - Phonons move against thermal gradient, as the system shifts away from thermal equilibrium
    - Push the electrons to one end through scattering

# Seebeck Effect

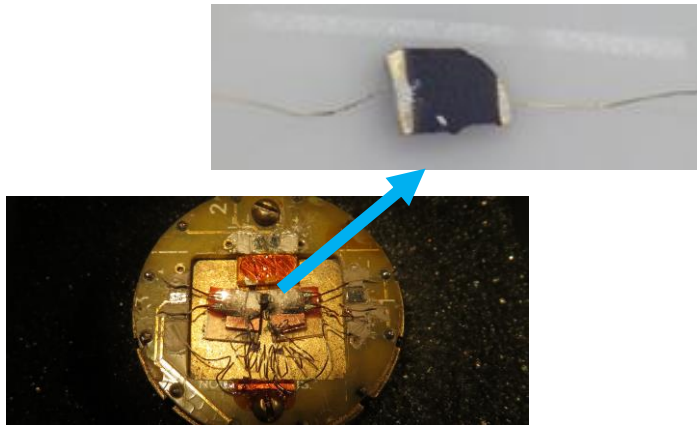
- Well established experimental evidence on the power law dependence of Seebeck coefficients on the in-plane hole concentration in hole-doped cuprates
- Implication on density of states of charge carriers.
- Relatively easy to set up compared to other experimental probes.



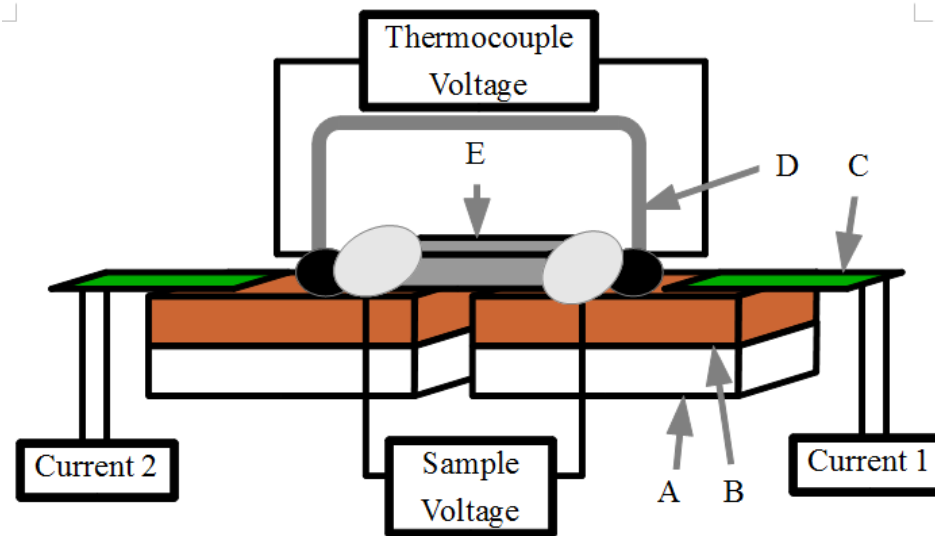
Seebeck coefficients of various hole-doped cuprates at 290K as a function of hole concentration per Cu-O plane  $P_{pl}$  for different types of hole-doped cuprates.

# Seebeck Coefficient Measurement

- Home-made setup: sample stage mounted on a standard Resistivity Puck for PPMS (Physical Property Measurement System)



A close-up photo of the Seebeck puck in this experiment.



Schematic diagram of Seebeck sample stage. A: Sapphire plates, B: Copper blocks, C: heater, D: Thermocouple, E: Sample. Copied from [6]

# Seebeck Coefficient Measurement

- Measurement done in PPMS
- Temperature cooled down from 300K to below  $T_c$  in certain temperature decrement
- Apply current to heater on one side after the temperature is stabilized
- Measure the voltage response of the sample
- Repeat the same measurement for the other heater
- Assume thermocouples and the sample are under the same  $\Delta T$ :

$$\frac{V_{sample}}{V_{thermocouple}} = \frac{S_{sample}}{S_{thermocouple}} = S_{relative}$$

# Results & Discussion

- Mott Formula for Seebeck Coefficient for weakly-interacting static system [8]:

$$S = \frac{\pi^2 k_B^2 T}{3e} \frac{d}{d\epsilon} [\ln \sigma(\epsilon)]_{\epsilon=\epsilon_F}$$

where  $\sigma(\epsilon)$  is the energy-dependent conductivity. Typically,

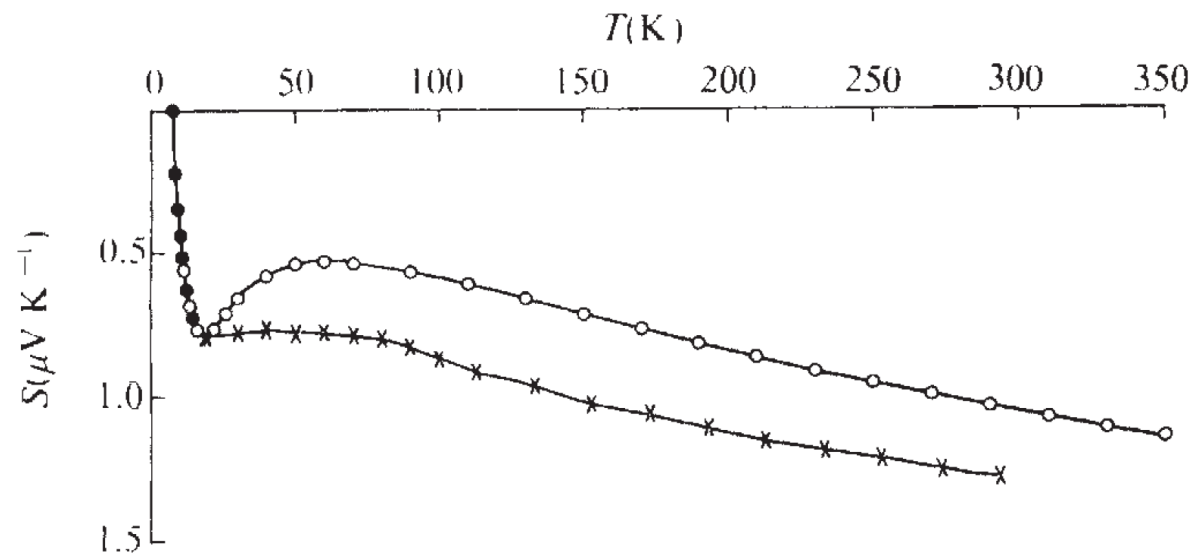
$$\frac{d}{d\epsilon} [\ln \sigma(\epsilon)]_{\epsilon=\epsilon_F} \sim \frac{1}{kT_F}$$

- For a simple metal,  $S \propto T$



# Results & Discussion

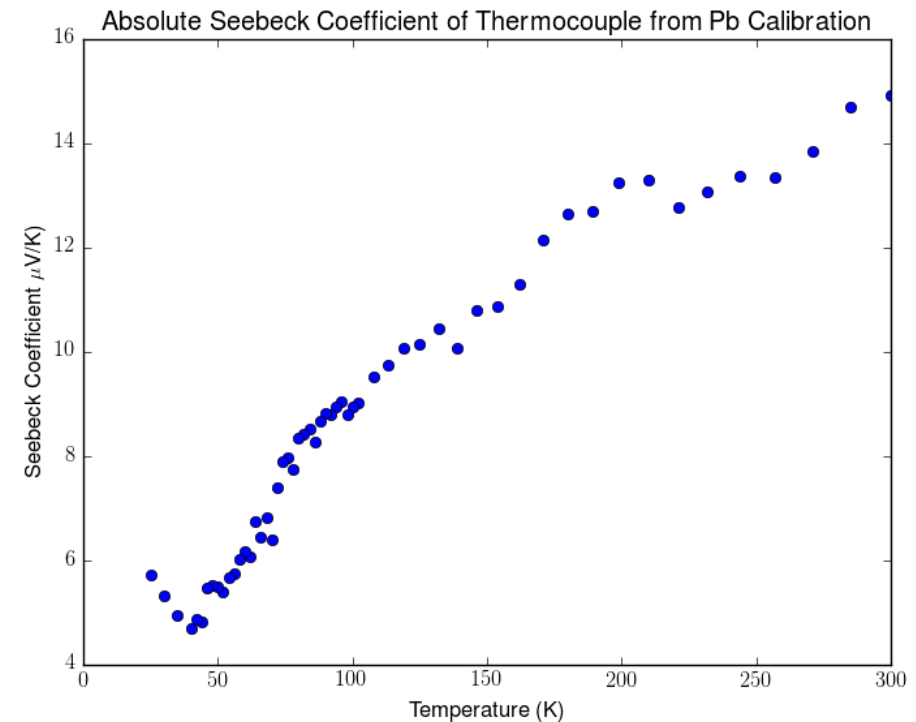
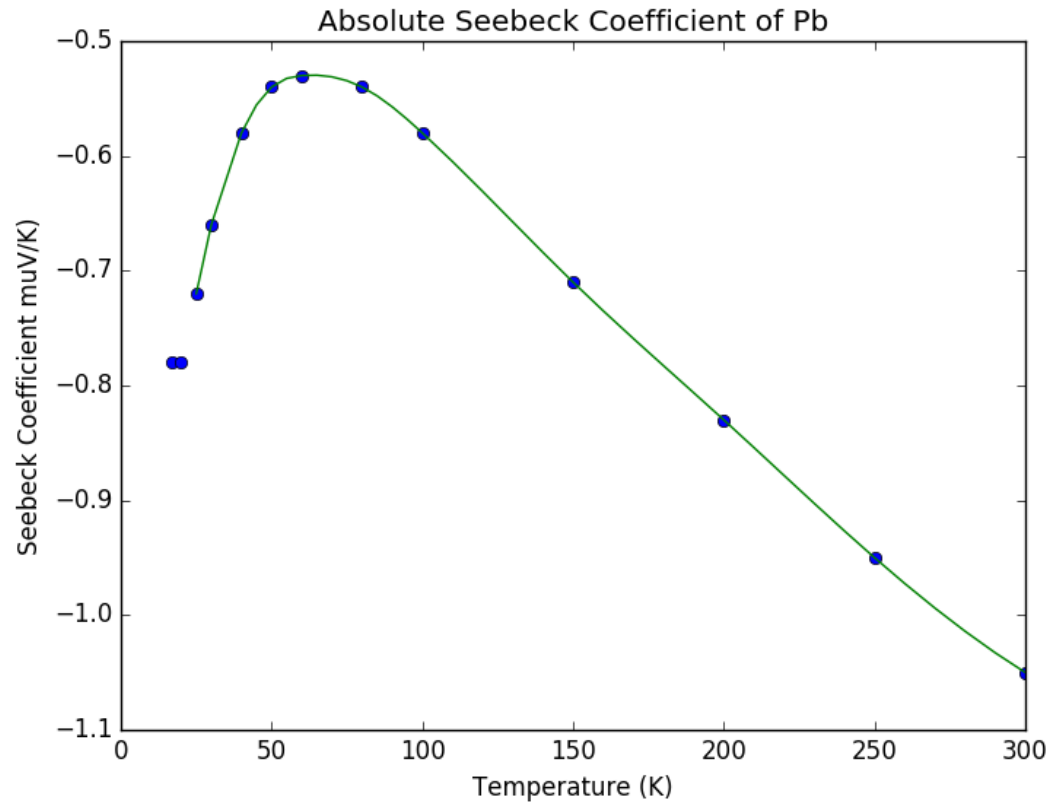
- Calibration with two different reference materials to find the absolute Seebeck coefficient of the thermocouple and the correction for the gold wires (which have finite seebeck coefficient). Pb and Pt are chosen.
- Seebeck coefficients of Pb [9].



X: Christian et. al 's  
compilation of Borelius'  
measurement  
O: R.B.Roberts'  
Measurement  
●: Christian et,al's  
measurement  
Copied form [13]

# Results & Discussion

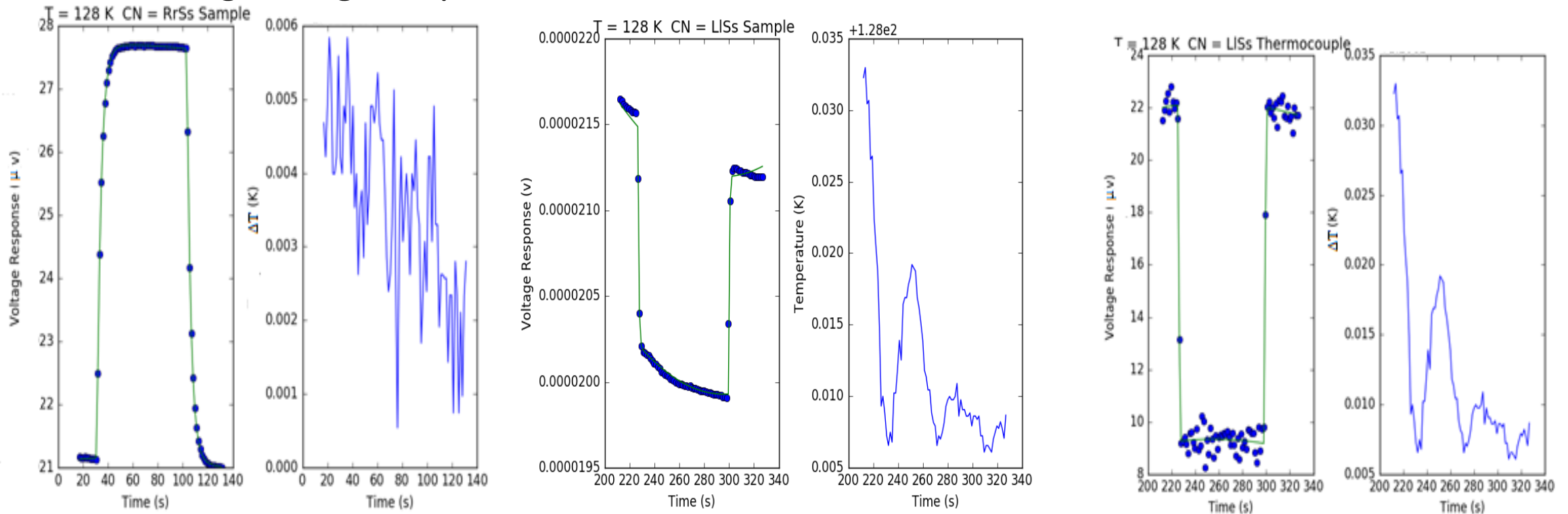
## Result from Pb Calibration



Result from Pt calibration diverges from expected behavior in the temperature range from 30K to 60K. Recalibration is needed.

# Results & Discussion

## Extracting voltage response

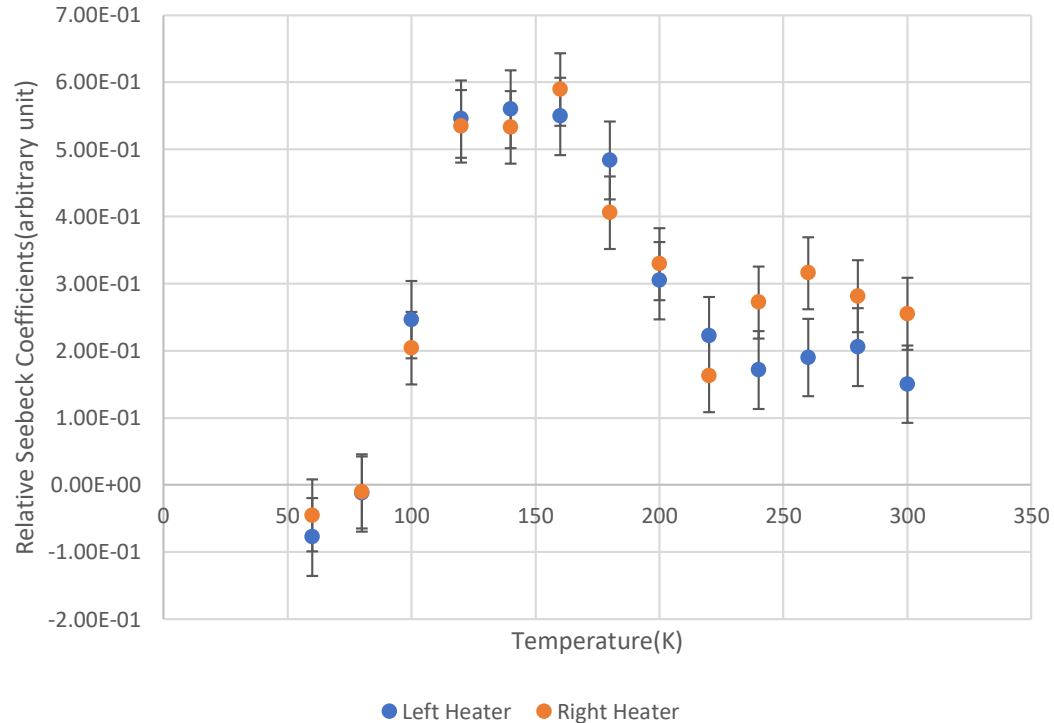


The plots on the left: fit to the response signal for sample and thermocouple at temperature 128K.

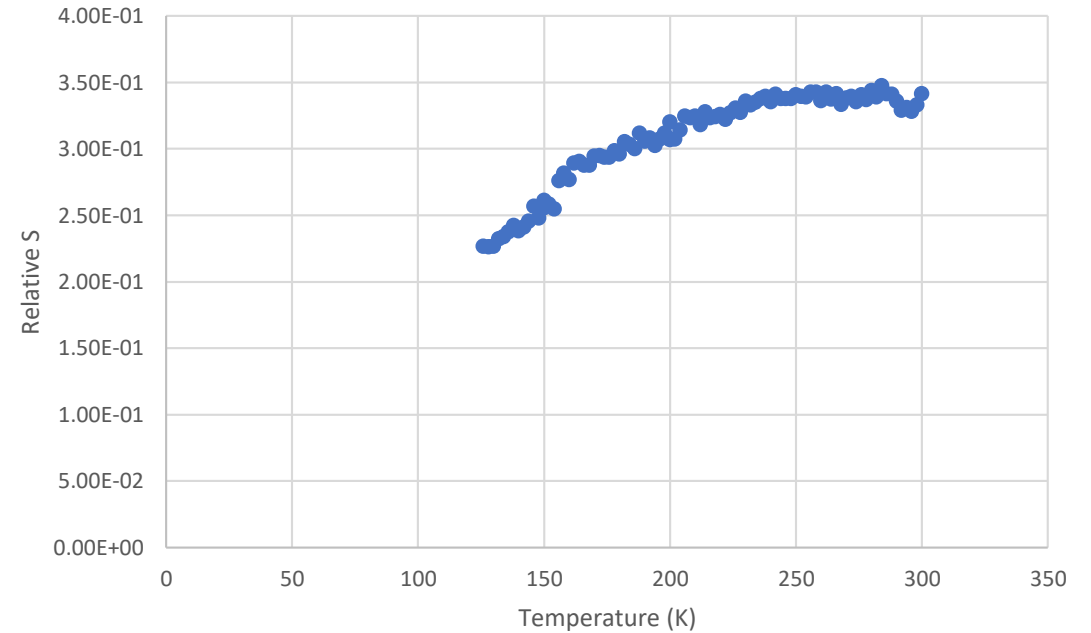
The plots on the right: Temperature fluctuation during the measurement.

# Results & Discussion

Relative Seebeck coefficients of two samples. The results of absolute



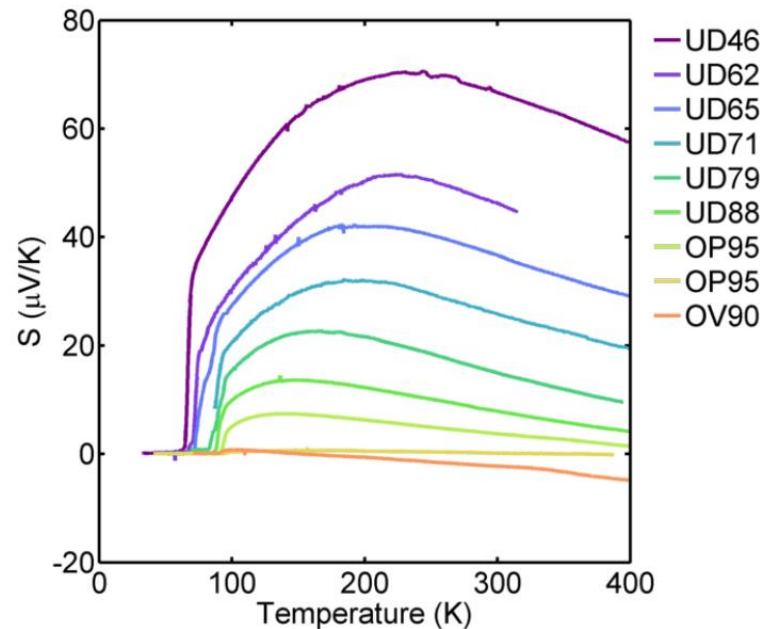
Relative Seebeck coefficients from test run of an as-grown sample  $T_c \approx 80\text{K}$



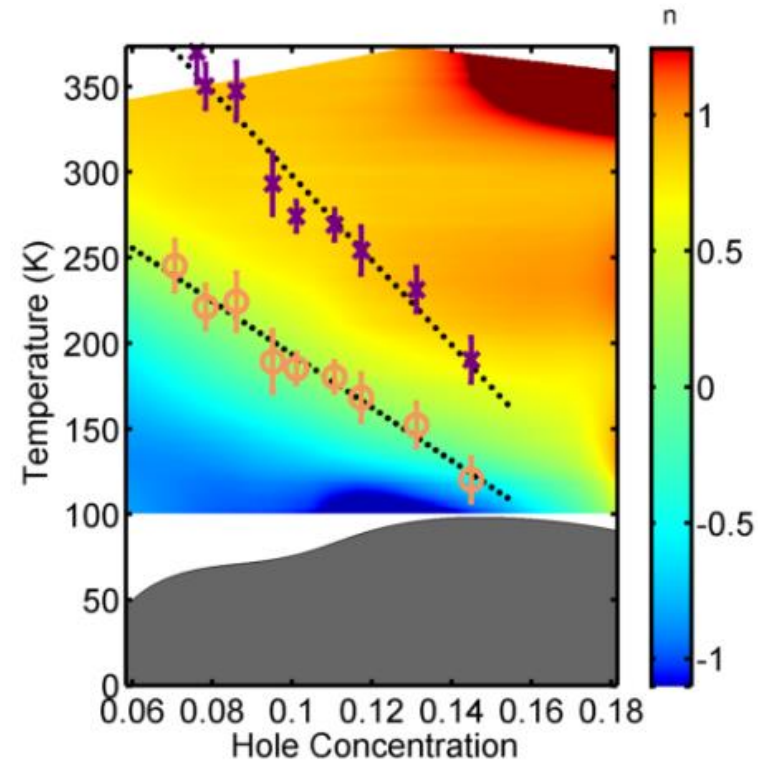
Relative Seebeck coefficients of an underdoped sample,  $T_c \approx 50\text{K}$

# Results & Discussion

- Results from Michael Veit [11]



Seebeck coefficients as a function of temperature for Hg1201 with different doping levels. Copied from [11]



The contour plot of the exponent  $n$  in the relation between  $S$  and  $T$ :  $S = AT^n + S_0$  in temperature-doping space. The area with grey shade represents the superconducting dome in this space. Copied from [11]

# Results & Discussion

- The low temperature behavior of Seebeck coefficient is quite surprising since it contains a linear term which obeys Mott formula for simple metal. This feature is present in the fermi liquid phase in the phase diagram for hole-doped cuprates, which suggests a hidden fermi liquid behavior in the pseudogap phase[10].
- The two characteristic temperatures labeled as circles and crosses in the contour plot in the previous slide also agree quite well with the characteristic temperatures obtained from resistivity measurement.

# Conclusion

- An approximately optimal Hg1201 growth condition for the current growth has been achieved
- Seebeck puck has been calibrated and all components worked as expected
- Ongoing Work:
  - Measure samples from a wide range of doping levels.
  - Second calibration with Pt in the temperature region 30~ 60K to determine the absolute Seebeck Coefficient of the sample.
- Future Direction
  - Consider better measurement techniques: AC heating current

# Acknowledgement

I want to thank Professor Greven for giving me the chance of working in the field of superconducting cuprates.

I would also like to thank Yang Tang, Zach Anderson, Vikram Nagarajan for their guidance and close collaboration.



# References

- [1] P.J. Ray, Master's thesis: Structural investigation of  $\text{La}(2-x)\text{Sr}(x)\text{CuO}(4+y)$  - Following staging as a function of temperature, (2016). doi:10.6084/m9.figshare.2075680.v2.
- [2] H.K. Onnes, The resistance of pure mercury at helium temperatures, *Commun Phys Lab Univ Leiden*. 12 (1911) .
- [3] HSC Physics Course Summary - From Ideas to Implementation, Dux Coll. (n.d.). <https://dc.edu.au/hsc-physics-ideas-to-implementation/> (accessed March 6, 2017).
- [4] J.G. Bednorz, K.A. Müller, Possible high  $T_c$  superconductivity in the Ba–La–Cu–O system, *Z. Für Phys. B Condens. Matter*. 64 (1986) 189–193. doi:10.1007/BF01303701.
- [5] H. Wen, Development of Research on New High Temperature Superconductors, *Development of Research on New High Temperature Superconductors*, *Chin. J. Mater. Res.* 29 (2015) 241–254. doi:10.11901/1005.3093.2015.111.
- [6] M.J. Veit, Transport Measurements of the Cuprate Superconductor  $\text{HgBa}_2\text{Cu}_{4+\delta}$ , University of Minnesota, 2014.
- [7] T. Honma, P.H. Hor, Unified electronic phase diagram for hole-doped high- $T_c$  cuprates, *Phys. Rev. B*. 77 (2008) 184520. doi:10.1103/PhysRevB.77.184520.
- [8] M. Jonson, G.D. Mahan, Mott's formula for the thermopower and the Wiedemann-Franz law, *Phys. Rev. B*. 21 (1980) 4223–4229. doi:10.1103/PhysRevB.21.4223.
- [9] R.B. Roberts, Absolute scale of thermoelectricity, *Nature*. 265 (1977) 226–227. doi:10.1038/265226a0.
- [10] N. Barišić, M.K. Chan, M.J. Veit, C.J. Dorow, Y. Ge, Y. Tang, W. Tabis, G. Yu, X. Zhao, M. Greven, Hidden Fermi-liquid behavior throughout the phase diagram of the cuprates, arXiv:1507.07885 [Cond-Mat]. (2015). <http://arxiv.org/abs/1507.07885> (accessed October 2, 2015).